Fig. 2 shows the measured on/off gain of the unit against pump power coupled into the DCF. At a pump power of 225mW, which was chosen as the operating point, the net gain is 1.4dB. A significant net gain can be obtained by increasing the pump power further, as seen in Fig. 2. However, double Rayleigh scattering in the 15.7km long fibre span will eventually impact the noise performance. Here, the objective was to demonstrate a nominally loss-free DCF module with a modest pump power which can be obtained from conventional semiconductor pump lasers.

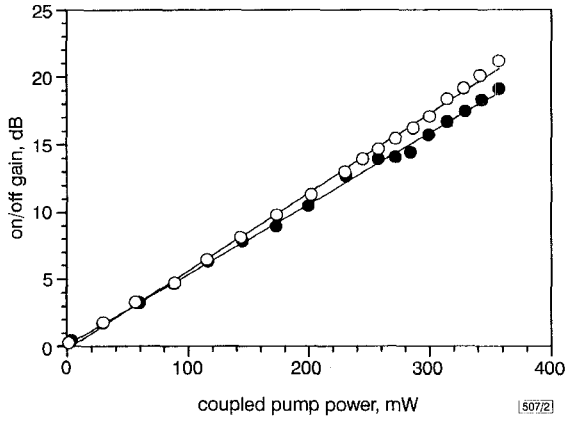

Fig. 2 *Measured net gain against pump power coupled into DCF*

Input powers are powers coupled into DCF
● input power : 0.04dBm
○ input power : –35dBm
——— linear fit

The performance of the DCF module was investigated in a 10Gbit/s transmission experiment. The transmitter is an externally modulated DFB laser with a wavelength of 1557.4nm generating a pseudo-random encoded optical bit stream with a word length of $2^{31}-1$ and a data rate of 9.953Gbit/s (OC-192). The receiver includes a conventional two-stage optical preamplifier combined with a saturating amplifier for limiting the optical signal incident on the PIN detector. The DCF module is inserted in front of the saturating amplifier. With a received signal of –35.8dBm, the input power to the DCF module is –1.4dBm (–2.3dBm into the DCF). The transmission fibre is a 71km long span of silica-core fibre with a loss of 13.2dB and a total dispersion of 1380ps/nm. The resulting net dispersion is –20ps/nm.

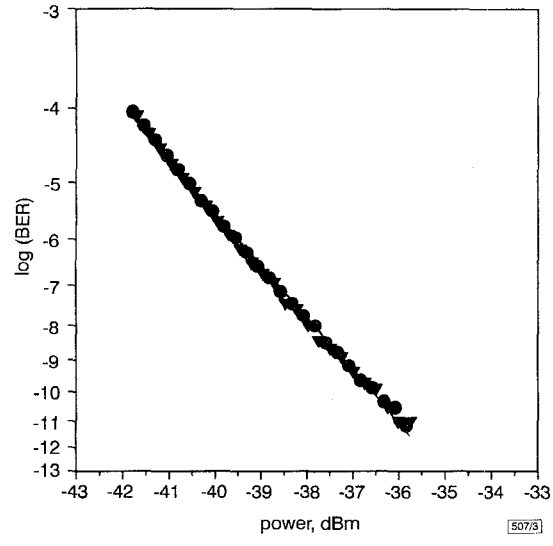

Fig. 3 *Measured BER against received power at 9.953 Gbit/s*

● back-to-back performance without DCF; baseline
▼ transmission through 71km of fibre with 1380ps/nm dispersion and Raman-DCF module in receiver
——— linear fit

Fig. 3 shows the measured bit error rates against received power. The triangles represent the results measured for transmission over the 71km fibre span combined with the dispersion-compensating module. The circles indicate the back-to-back performance (0km transmission distance and no DCF module in the receiver). Both sets of data show a sensitivity of –37.2dBm for a bit error rate of 10^{-9}, indicating penalty-free operation of the DCF module.

In conclusion, we have demonstrated that Raman gain can be exploited to offset the insertion loss of dispersion-compensating fibre modules without incurring penalties in system performance. The required pump powers are very modest due to the small mode-field diameter of typical dispersion-compensating fibres.

23 March 1998
Electronics Letters Online No: 19980756

P.B. Hansen (*Bell Laboratories, Lucent Technologies, 101 Crawfords Corner Road, Holmdel, NJ 07733, USA*)

E-mail: pbh@bell-labs.com

G. Jacobovitz-Veselka (*Network Systems, Lucent Technologies, 25 Schoolhouse Road, Somerset, NJ 08873, USA*)

L. Grüner-Nielsen (Lucent Technologies Denmark, Priorparken 680, DK-2605, Brøndby, Denmark)

A.J. Stentz (*Bell Laboratories, Lucent Technologies, 600 Mountain Avenue, Murray Hill, NJ 07974, USA*)

References

1 DUGAN, J.M., PRICE, A.J., RAMADAN, M., WOLF, D.L., MURPHY, E.F., ANTOS, A.J., SMITH, D.K., and HALL, D.W.: 'All-optical, fiber-based 1550nm dispersion compensation in a 10Gbit/s, 150km transmission experiment over 1310nm optimised fiber'. Proc. Optical Fiber Communication Conf., 1992, Paper PD-14, pp. 367–370

2 HANSEN, P.B., ESKILDSEN, L.E., GRUBB, S.G., VENGSARKAR, A.M., KOROTKY, S.K., STRASSER, T.A., ALPHONSUS, J.E.J., VESELKA, J.J., DIGIOVANNI, D.J., PECKHAM, D.W., BECK, E.C., TRUXAL, D.A., CHEUNG, W.Y., KOSINSKI, S.G., GASPER, D., WYSOCKI, P.F., DA SILVA, V.L., and SIMPSON, J.R.: '2.488-Gb/s unrepeatered transmission over 529km using remotely pumped post- and pre-amplifiers, forward error correction, and dispersion compensation'. Proc. Optical Fiber Communication Conf., 1995, Paper PD-25

3 GRUBB, S.G., A, S.T., CHEUNG, W.Y., REED, W.A., MIZRAHI, V., ERDOGAN, T., LEMAIRE, P.J., and VENGSARKAR, A.M.: 'High-power 1.48μm cascaded Raman laser in germanosilicate fibers'. Proc. Topical Meeting on Optical Amplifiers and Their Applications, 1995, Paper SaA4, pp. 197–199

Spectral tailoring of erbium superfluorescent fibre source

S.D. Dyer and K.B. Rochford

The output spectrum of an erbium superfluorescent fibre source (SFS) is tailored by replacing the broadband mirror in the conventional double-pass design with a combination of reflective Bragg gratings. Increased bandwidth and a factor of two reduction in coherence length are demonstrated compared to a conventional SFS.

Introduction: The erbium superfluorescent fibre source (SFS) provides a high-power, broadband, fibre-coupled output signal [1]. However, the output spectrum of the erbium SFS is usually very nonuniform [1], and this leads to undesirable effects in the coherence function of the source, such as side-lobes in the coherence function and increased coherence length.

In this Letter, we demonstrate a novel method for tailoring the SFS spectrum by incorporating one or more fibre Bragg gratings (FBGs) in a double-pass configuration. Previous work has suggested that narrow (0.1nm) spectral features can be boosted with Bragg grating reflectors to produce a multiwavelength source for wavelength-division multiplexing [2]. We show that wavelength-selective feedback can also be used to tailor the output spectrum when the correct combination of reflective Bragg gratings is included in the source configuration. This tailoring can give a flattened spectrum, reduced coherence length, or other useful features. The spectrally tailored SFS has many applications, including low-coherence interferometry and optical component testing.

Design: Our SFS source configuration is a modification of the conventional backward-signal, double-pass configuration, as shown in Fig. 1. Instead of a broadband mirror, a combination of Bragg gratings is used as a wavelength-selective reflector at the unpumped end of the erbium fibre. This creates a device that is double-pass for some wavelengths and single-pass for others. The spectrum of the output light is tailored by selecting Bragg gratings with the appropriate centre wavelength, bandwidth, and reflectance. For example, a combination of Bragg gratings can be chosen to provide reflection at those wavelengths where the output power is low. The reflected light experiences additional amplification as it propagates through the erbium fibre a second time. In this manner, the spectrum of the output light is equalised and the spectral nonuniformity minimised.

In contrast to simple output filtering to obtain a specific spectral shape, the Bragg reflectors select a specific wavelength band for amplification, and excited-state erbium ions are not wasted in amplifying undesired wavelengths [3]. This effectively redistributes gain and maximises output power across the desired band.

Lasing induced by backreflections can be a significant problem in the design of a double-pass SFS. However, this problem can be avoided through the inclusion of an isolator at the output end of the source and careful splicing of the erbium fibre to the WDM fibre.

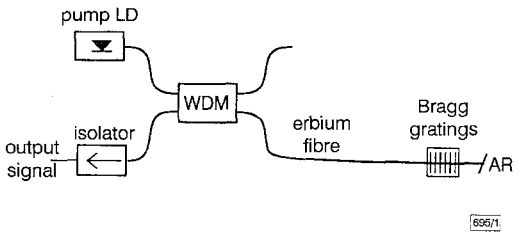

Fig. 1 *Double-pass SFS with reflective Bragg gratings for spectral tailoring*

WDM: wavelength-division multiplexer; AR: anti-reflection medium

Results: We constructed a double-pass SFS as shown in Fig. 1. A high-power 980nm laser diode was used as the pump source, and a 13m length of aluminosilicate fibre doped with 250ppm of erbium was chosen as the active medium. A broadband Bragg grating, with a central wavelength of 1548.5nm and 93% reflectance over its 26nm bandwidth, was fusion spliced to the unpumped end of the erbium fibre. The reflectance spectrum of this FBG is shown in Fig. 2. The Bragg grating boosts the power in the longer wavelengths of the output spectrum, so that the spectrum is now approximately uniform, as shown in Fig. 2. At high pump powers, such as the 107mW pump power used for Fig. 2, the spectral shape is independent of the exact pump power. However, at extremely low pump powers, most of the power is absorbed before reaching the Bragg gratings, and the Bragg gratings have little effect on the output spectrum.

To compare the spectrum of the double-pass source to the corresponding spectrum generated by a single-pass source, we broke the splice connecting the erbium fibre and the Bragg grating, and immersed the bare end of the erbium fibre in index-matching fluid to prevent backreflections. The spectrum of the single-pass source is shown in Fig. 2. The double-pass FBG configuration yields an increase of > 10dB throughout the longer wavelength portion of the spectrum, and provides a 27nm spectrum with ±3dB variation.

The measured output power as a function of the pump power for both the single-pass and the double-pass configurations is shown in Fig. 3. In either configuration, the total output power is an approximately linear function of pump power above threshold. The 28% slope efficiency of the spectrally tailored double-pass source is more than double the 12% slope efficiency of the single-pass design.

The double-pass SFS with spectral tailoring is particularly useful for reducing coherence length. The fringe visibilities as a function of path length difference were calculated from the measured spectra and are shown in Fig. 4. The coherence length l_c was calculated for the two sources from the definition

$$l_c = c\int_{-\infty}^{\infty} |\gamma(\tau)|^2\, d\tau \qquad (1)$$

where $\gamma(\tau)$ is the complex degree of coherence [4]. The coherence length of the spectrally tailored double-pass source is 93μm, approximately half the 193μm coherence length of the conventional single-pass design.

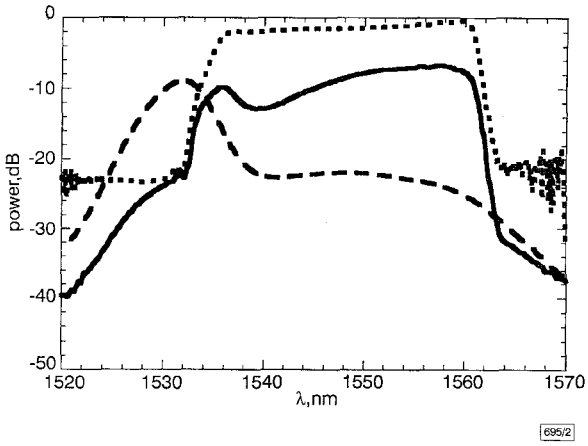

Fig. 2 *Output spectra of conventional single-pass SFS and spectrally tailored double-pass SFS with reflectance spectrum of FBG used in double-pass device*

····· FGB reflectance spectrum
– – – – single-pass SFS spectrum
——— spectrally tailored double-pass SFS spectrum

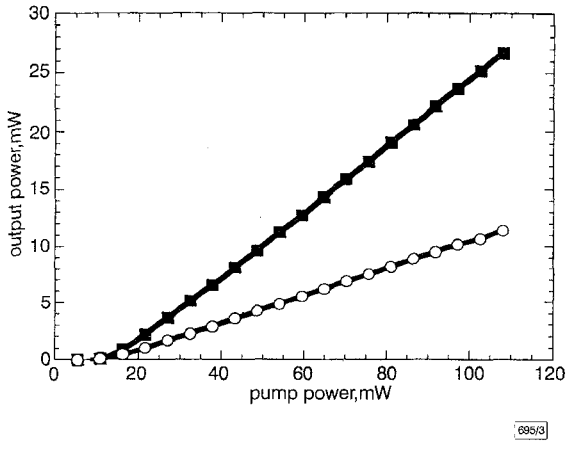

Fig. 3 *Output power against pump power for conventional single-pass SFS and spectrally tailored double-pass SFS*

—○— single-pass SFS
—■— spectrally tailored double-pass SFS

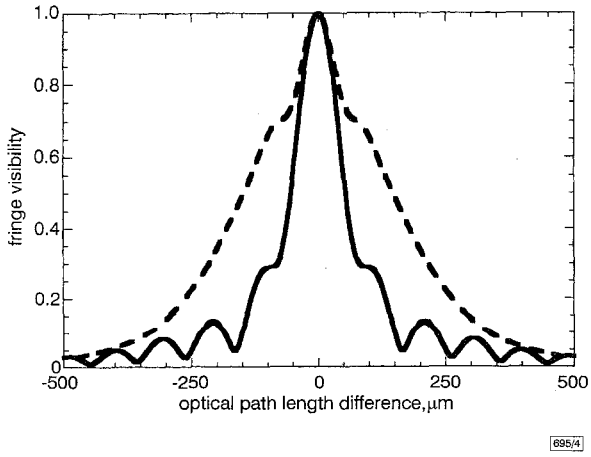

Fig. 4 *Fringe visibility curves of conventional single-pass SFS and spectrally tailored double-pass SFS*

– – – – single-pass SFS
——— spectrally tailored double-pass SFS

Conclusions: Our method of tailoring the spectrum of an SFS uses a combination of Bragg gratings as wavelength-selective reflectors to create a double-pass device. The output spectrum of the source

can be dramatically modified by this method. Although our results were achieved using a broadband Bragg grating with a flat reflectance spectrum, further tailoring of the spectrum can be achieved using a combination of Bragg gratings with specially tailored reflectance profiles. The key advantage of this design is its flexibility; the spectrum can be tailored to meet the needs of many applications simply by choosing the appropriate Bragg gratings.

27 November 1997

Electronics Letters Online No: 19980748

S.D. Dyer and K.B. Rochford (*National Institute of Standards and Technology, Optoelectronics Division, 325 Broadway, Boulder, CO 80303, USA*)

E-mail: sdyer@boulder.nist.gov

References

1 WYSOCKI, P.F., DIGONNET, M.J.F., KIM, B.Y., and SHAW, H.J.: 'Characteristics of erbium-doped superfluorescent fiber sources for interferometric sensor applications', *J. Lightwave Technol.*, 1994, **12**, (3), pp. 550–567

2 HUBER, D.R.: 'Narrow band incoherent optical carrier generator'. US Patent No. 5,191,586, March 1993

3 TACHIBANA, M., LAMING, R.I., MORKEL, P.R., and PAYNE, D.N.: 'Erbium-doped fiber amplifier with flattened gain spectrum', *IEEE Photonics Technol. Lett.*, 1991, **3**, (2), pp. 118–120

4 GOODMAN, J.W.: 'Statistical optics' (John Wiley & Sons, Inc., 1985)

Ultrasonic field and temperature sensor based on short in-fibre Bragg gratings

N.E. Fisher, D.J. Webb, C.N. Pannell, D.A. Jackson, L.R. Gavrilov, J.W. Hand, L. Zhang and I. Bennion

The authors demonstrate that in-fibre Bragg gratings may be successfully used to measure megahertz acoustic fields if the grating length is sufficiently short and the optical fibre is appropriately desensitised. A noise-limited pressure resolution of 4.5×10^{-3}atm/√Hz was found. The capability to simultaneously act as a temperature sensor is also demonstrated.

Introduction: There is a need for assessment of the safety of ultrasound for medical applications due to the trend towards increasing output powers from diagnostic ultrasound equipment and the widening use of high intensity ultrasonic fields in a range of therapeutic applications (e.g. [1]). Conventional probes use the piezoelectric effect, but such devices suffer from a susceptibility to electromagnetic interference, signal distortion and lack of multiplexing capability. To overcome these 'electrical' problems, several approaches utilising optical fibres based on interferometric and polarimetric techniques have been described (e.g. [2, 3]).

In this Letter, we demonstrate that short in-fibre Bragg gratings (FBG) may also be used to detect high frequency (megahertz) ultrasonic fields. These devices offer distinct advantages such as small diameter, ease of multiplexing, simultaneous measurement of temperature, and potentially low cost.

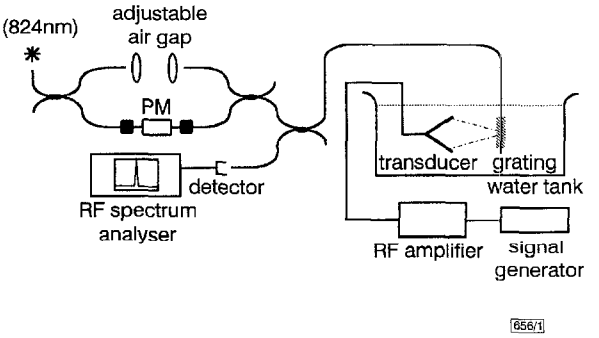

Fig. 1 *Experimental arrangement*

PM = phase modulator

Experiment: The arrangement used to interrogate the grating is shown in Fig. 1. Light from a 1mW pig-tailed superluminescent diode centred at 824nm with a bandwidth of ≃ 42nm was launched into an unbalanced Mach-Zehnder interferometer (MZI). Incorporated in one arm of the MZI was a phase modulator to frequency shift the light and thus allow the use of pseudo-heterodyne signal processing [4].

Provided that the optical path difference between the MZI's arms is longer than the source coherence length and shorter than the effective coherence length of the back-reflected light from the grating, an interference signal is observed which is in the form of (in the absence of grating strain) a carrier produced by the phase modulator. Strain-induced changes in the Bragg wavelength then induce a corresponding phase modulation of the carrier which we measured by determining the amplitudes of the resulting upper and lower side-band frequency components observed on a radio frequency RF spectrum analyser. The grating had a nominal Bragg wavelength of 820nm, a bandwidth of 0.2nm, a reflectivity of 80%, and a length of 5mm. The transducer was driven continuously in water at its resonant frequency of 1.911MHz, and generated a maximum acoustic pressure of ≃ 2atm (measured using a calibrated PVDF hydrophone) in an acoustical focal spot of radius ≃ 1 – 2mm.

Results for 5mm grating: We observed two anomalies in the response of the grating to the ultrasonic field: (i) an asymmetry in the magnitudes of the side-band components and (ii) a large homodyne signal at 1.911MHz. We repeated these experiments using sound waves ranging from 100Hz (FBG in air) up to 76kHz (FBG in water). In these cases, we observed the expected system response; hence the anomalies stem from the use of high frequency ultrasound. Now consider Fig. 2 (top), which shows a typical side-band response (normalised to its carrier) with displacement, following a scan of the focal spot along the FBG/fibre. Note that the system response extends over a distance that is *much greater* than the grating length and is *periodic*. Hence, as we reported in [5], we conclude that compressional standing waves (which can extend many centimetres) are set up by the ultrasound in the fibre (although they are attenuated by the acrylic jackets which are on either side of the grating). Since these waves must only partially modulate the FBG, as their length (3.1mm in the case of 1.911MHz) is less than the grating length, this means that the grating is subject to a *nonuniform* strain which leads to regions of the grating acting as spectral filters for the back-reflected light from other regions of the grating. Our conjecture is that this gives rise to the amplitude modulation (the homodyne signal) which modifies the interferometric signals leading to the asymmetric side-bands.

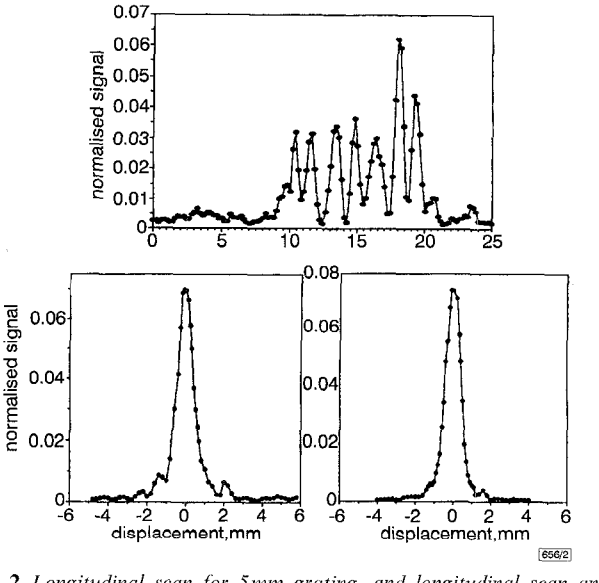

Fig. 2 *Longitudinal scan for 5mm grating, and longitudinal scan and lateral scans for shielded 1mm grating*

Top: longitudinal scan for 5mm grating
Bottom: longitudinal (left) and lateral (right) scans for shielded 1mm grating